AD-A039 944 STANFORD UNIV CALIF INST FOR PLASMA RESEARCH F/G 3/2
FORCE FREE MAGNETIC FIELDS AND SOLAR ACTIVITY.(U)
DEC 76 P A STURROCK, C W BARNES F19628-74-C-0054
UNCLASSIFIED AFGL-TR-77-0023 NL

| OF |
AD
A039944

END

DATE
FILMED
6-77

AFGL-TR-77-0023

FORCE FREE MAGNETIC FIELDS AND SOLAR ACTIVITY

P.A. Sturrock
C.W. Barnes

Institute for Plasma Research
Stanford University
Via Crespi
Stanford, California 94305

December 1976

Final Report

(1 July 1974 - 31 December 1976)

Approved for public release; distribution unlimited.

AIR FORCE GEOPHYSICS LABORATORY
AIR FORCE SYSTEMS COMMAND
UNITED STATES AIR FORCE
HANSCOM AFB MASSACHUSETTS 01731

UNCLASSIFIED

SECURITY CLASSIFICATION OF THIS PAGE (When Data Entered)

REPORT DOCUMENTATION PAGE

READ INSTRUCTIONS BEFORE COMPLETING FORM

1. REPORT NUMBER: AFGL-TR-77-0023

2. GOVT ACCESSION NO.

3. RECIPIENT'S CATALOG NUMBER

4. TITLE (and Subtitle): FORCE FREE MAGNETIC FIELDS AND SOLAR ACTIVITY

5. TYPE OF REPORT & PERIOD COVERED: Final Report. 1 Jul 1974-31 December 1976.

6. PERFORMING ORG. REPORT NUMBER

7. AUTHOR(s): P.A. Sturrock and C.W. Barnes

8. CONTRACT OR GRANT NUMBER(s): F19628-74-C-0054

9. PERFORMING ORGANIZATION NAME AND ADDRESS
Institute for Plasma Research
Stanford University
Via Crespi, Stanford, California 94305

10. PROGRAM ELEMENT, PROJECT, TASK AREA & WORK UNIT NUMBERS: 7649-06-01 62101F

11. CONTROLLING OFFICE NAME AND ADDRESS
Air Force Geophysical Laboratory
Hanscom AFB, Massachusetts 01731
Contract Monitor: John W. Evans/LM

12. REPORT DATE: December 1976

13. NO. OF PAGES: 27

15. SECURITY CLASS. (of this report): Unclassified

14. MONITORING AGENCY NAME & ADDRESS (if diff. from Controlling Office)

15a. DECLASSIFICATION/DOWNGRADING SCHEDULE

16. DISTRIBUTION STATEMENT (of this report)

Approved for public release; distribution unlimited

17. DISTRIBUTION STATEMENT (of the abstract entered in Block 20, if different from report)

18. SUPPLEMENTARY NOTES

Tech. other

19. KEY WORDS (Continue on reverse side if necessary and identify by block number)

Force-free fields
Solar flares
Solar magnetic fields

20. ABSTRACT (Continue on reverse side if necessary and identify by block number)

This study, aimed at the prediction of solar flares, centers on devising methods for calculating magnetic field structures in the solar atmosphere. Force-free fields comprise an important class of magnetic-field structures which may be calculated by relaxation techniques. Models under active consideration involve spherical boundary surfaces and cylindrical symmetry. Study of the energy of such field configurations indicates that, for sufficiently large shear, force-free fields will be unstable against perturbations leading to eruption. The condition for this instability and the mechanism of instability have been investigated. The studies are related to erupting prominences and coronal transients, as well as solar flares.

DD FORM 1 JAN 73 1473

EDITION OF 1 NOV 65 IS OBSOLETE

UNCLASSIFIED

SECURITY CLASSIFICATION OF THIS PAGE (When Data Entered)

FORCE FREE MAGNETIC FIELDS AND SOLAR ACTIVITY

I. INTRODUCTION

The key phenomenon of solar activity is the solar flare, and it is generally agreed that the energy released in a solar flare is derived from magnetic energy (Sweet, 1969). The structure of magnetic-field configurations in the solar atmosphere is therefore essential for understanding solar activity in general and solar flares in particular. One meaningful way to approach the problem of flare prediction is to develop methods for determining magnetic-field configurations in active regions and to find procedures for predicting the evolution of these configurations. Since the pressure of the coronal plasma is less than the magnetic stress in active regions, the magnetic field in solar active regions typically comprises one of two configurations. One of these is the "force-free" state (Schmidt, 1968), and the other is the "current sheet". It is widely believed that the current sheet plays a key role in the flare process since the "Petschek mechanism" (Petschek, 1964) constitutes a rapid mode for the release of free magnetic energy. Our studies of solar flares (Barnes and Sturrock, 1972) indicate that the transformation of a force-free configuration into a current-sheet configuration may be a key step in the overall flare process.

More recent work by Spicer (1976) leads to a flare model in which the free magnetic energy is the excess energy of a force-free field configuration. In the Spicer model, rapid energy release becomes possible through a resistive-type instability, comparable with the

"tearing-mode instability" (Furth, Killeen and Rosenbluth, 1963) which leads to rapid energy release from current sheets.

For the above reasons, it is essential that one be able to compute force-free magnetic-field structures if one is to make detailed analysis of magnetic-field changes which lead to solar flares. This is true either for a short-term goal or a long-term goal. The short-term goal is simply that of developing magnetic-field models which are simple enough for detailed study, but which bear some relation to magnetic-field patterns likely to arise in the sun's atmosphere. The long-term goal is that of computing magnetic-field structures in the sun's atmosphere based on study of the observed magnetic-field configuration of the photosphere and the photospheric velocity field. The latter involves the calculation of force-free magnetic-field configurations in three dimensions which is beyond the capability of the computer now available to us. For this reason, we have limited our scope to the study of model force-free magnetic-field configurations in two dimensions.

II. SPECIFIC GOALS

Our first goal was that of developing computational procedure for the calculation of force-free magnetic-field configurations. The relevant equation is

$$\vec{j} \times \vec{B} = 0 \tag{2.1}$$

and

$$\nabla \times \vec{B} = 4\pi\vec{j} \tag{2.2}$$

so that equation (2.1) may be rewritten as

$$\vec{B} \times (\nabla \times \vec{B}) = 0 \quad . \tag{2.3}$$

It follows from this euqation that

$$\nabla \times \vec{B} = \varkappa \vec{B} \tag{2.4}$$

where $\varkappa(\vec{x})$ is a scalar function of position. However, on operating on both sides of this equation with the gradient operator and noting that

$$\nabla \cdot \vec{B} = 0 \quad , \tag{2.5}$$

we find that

$$\vec{B} \cdot \nabla \varkappa = 0 \tag{2.6}$$

so that $\varkappa$ is a constant along any field line. In general, however, $\varkappa$ will vary from one field line to the next.

If one considers the restricted class of force-free magnetic-field configurations for which $\varkappa$ = const., the governing equation (2.4) is a <u>linear</u> equation. This is a great simplification in computing field configurations and it is one which has been used extensively in the investigation of force-free fields. However, there is no <u>a priori</u> reason to expect that a real magnetic-field configuration occurring in the sun's atmosphere will have $\varkappa$ = constant. For instance, if we consider the magnetic-field configuration produced by a localized current distribution, we may expect that it will vary with distance L asymptotically as a power law:

$$|B| \propto L^{-n} \quad . \tag{2.7}$$

This means that

$$(\nabla \times B) \propto L^{-n-1} \tag{2.8}$$

so that

$$|\varkappa| \propto L^{-1} \quad . \tag{2.9}$$

It can, in fact, be shown that a magnetic-field configuration constrained to have $\varkappa$ = constant over an infinite volume will have infinite energy (Anzer, 1976).

The procedure which we have developed at Stanford for the study of force-free magnetic-field configurations, without the restriction $\varkappa$ = constant, is based on the representation

$$B = \nabla\alpha \times \nabla\beta \tag{2.10}$$

which follows from equation (2.5). One readily verifies that

$$B \cdot \nabla\alpha = 0 \ , \qquad B \cdot \nabla\beta = 0 \quad , \tag{2.11}$$

so that both α and β are constant along any field line. Hence we see also that

$$(\nabla \times B) \cdot \nabla\alpha = 0 \ , \qquad (\nabla \times B) \cdot \nabla\beta = 0 \quad , \tag{2.12}$$

which may be rewritten as

$$\nabla\alpha \cdot [\nabla \times (\nabla\alpha \times \nabla\beta)] = 0 \tag{2.13}$$

$$\nabla\beta \cdot [\nabla \times (\nabla\alpha \times \nabla\beta)] = 0 \quad . \tag{2.14}$$

These may be expressed in diadic notation as follows

$$(\nabla\beta)^2\,\nabla^2\alpha - \nabla\beta\nabla\beta:\nabla\nabla\alpha - (\nabla\alpha.\nabla\beta)\nabla^2\beta + \nabla\alpha\nabla\beta:\nabla\nabla\beta = 0 \qquad (2.15)$$

$$- (\nabla\alpha.\nabla\beta)\nabla^2\alpha + \nabla\alpha\nabla\beta:\nabla\nabla\alpha + (\nabla\alpha)^2\nabla^2\beta - \nabla\alpha\nabla\alpha:\nabla\nabla\beta = 0 \quad . \qquad (2.16)$$

These equations are in fact suitable for numerical calculation by the relaxation procedure. This is equivalent to determining whether, for a given assumed field configuration, $\vec{j} \times \vec{B}$ vanishes at a particular point and, if it does not, allowing the field line to adjust itself to make $\vec{j} \times \vec{B} = 0$ locally.

The principal aim of this research program has been to study models of force-free magnetic-field configurations using the representation (2.10) and the relaxation procedure for numerical computation.

III. RESULTS

In order to make the models sufficiently simple to calculate, it is essential to introduce some kind of symmetry. It is possible to develop field models using translational symmetry in terms of a rectangular coordinate system, as was done some years ago (Sturrock and Woodbury, 1967). However, such field patterns can never erupt to form current sheets since an open field pattern based on a line dipole has infinite energy per unit length. It is therefore essential to go to a more realistic geometry such as cylindrical geometry or spherical geometry.

When force-free field patterns of cylindrical symmetry were first investigated (Barnes and Sturrock, 1972), we found that the total energy in the magnetic field configuration increases progressively

with angle of shear, and that, for shear angles above some critical value (about π), the energy in the magnetic field exceeds the energy of the corresponding open-field configuration. This then led to the important possibility that a force-free magnetic-field configuration might, if sufficiently stressed, become unstable against an "eruptive instability" which develops the field pattern into an open configuration involving a current sheet. This current sheet could then provide further energy release by field-line reconnection (Petschek, 1964), which is the probable mechanism for energy release in solar flares.

One of the main aims of this research program has been to further investigate model force-free magnetic-field patterns, extending the geometry to the more realistic spherical geometry. It was important to determine whether the energy property just mentioned is common to all force-free configurations or whether it applies only to some special class of such configurations.

We faced a number of problems in pursuing this aim. One real handicap was the limited capability of the Stanford computer which made it necessary to work with a much coarser mesh than is desirable. Another difficulty was that of obtaining convergence of the relaxation procedure. It is essential to introduce a "relaxation parameter" λ defined by

$$\vec{B}^{(n+1)} = (1 - \lambda)\, \vec{B}^{(n)} + \lambda\, B_{est.}^{(n)} \qquad (3.1)$$

where $\vec{B}^{(n)}$ is the field pattern obtained by the n'th iteration and $B_{est.}^{(n)}$ is the field pattern indicated by "full" relaxation, adjusting each mesh point in turn (or in blocks) to satisfy the equations (2.15)

and (2.16). As the field became progressively more stressed, it was necessary to use a smaller and smaller value of λ to insure convergence. Unfortunately, this means that the convergence became slower and slower.

Since there were no simple analytical models, based on spherical geometry, against which to test our code, a minor error persisted in the code for some time.

An example of our calculation of force-free field configurations, based on a spherical boundary, is shown in Figures 3.1 - 3.3. It is assumed that the field pattern has cylindrical symmetry above the axis of the spherical coordinate system and this leads to the representation (2.10) for which $\alpha = \alpha(r,\theta)$ and

$$\beta = \varphi - \gamma(r,\theta) \quad . \tag{3.2}$$

Contours of constant α give the field lines themselves, since α is a measure of magnetic flux enclosed in a circle with constant values of r and θ. Contours of constant γ give the shear angle of the field line. In fact, it was convenient to use log r rather than r as the radial variable. This leads to a mesh which is finer in the high-field regions and coarser in the weak-field regions. It was assumed that α and γ are prescribed along the surface of the sphere.

An additional difficulty in our calculations concerned the choice of outer boundary. (In principal, we would have wished that we could dispense with an outer boundary and extend the field pattern to infinity.) It was, however, convenient to introduce an outer boundary which was perfectly conducting. Field lines can therefore not penetrate the limits of the computational mesh. If the outer radius of the system

could be chosen large enough, one could hope that the conducting boundary would appear to the field to be lying at infinity. Then the exact form of boundary conditions chosen for the outer spherical boundary would not be important.

We found, however, that as the field shear was increased, a point was reached at which the fields seemed to billow out rapidly (as a function of rate of increase of shear, not time) and to press against the outer boundary. This readily occurred even though the outer boundary was placed as far out as 700 surface radii. In comparing the energy stored in the fields, under various conditions of shear, with the energy stored in a completely open field configuration (current free, except for a current sheet region), it was observed that, as the shear was increased, increasing the stored energy in the system, the lines billowed out before the stored energy reached the equivalent open field energy. This implies that there is a smooth transition between closed and open field configurations in the spherical model, with no build-up of excess stored energy as shear increases. Figures 3.1 - 3.3 show some typical field configurations for surface shear angles of 2.6, π and 2π radians, respectively. The boundaries are at $\theta = 0$ and $\pi/2$ and $R/R_0 = 1$ and 180. The boundary at $R/R_0 = 180$ is taken to be open (approximated by allowing field lines to pass through the boundary with the condition that they be straight there). The equatorial boundary ($\theta = \pi/2$) is taken to be conducting, as if a mirror image existed in the southern hemisphere. One can see in Figure 3.1 (maximum shear = 2.6 radians) that the field lines bulge outward to a fairly large radius, but do not seem to sense the presence of the outer boundary (the field configuration for this shear angle

is observed to be the same for both open and closed outer boundaries). Figure 3.2 shows the fields for a shear of π radians. Here, the fields extend beyond the boundary. Then, in Figure 3.3 (shear = 2π radians), the fields extend outward even further. The total stored energy increases only slowly with increasing shear, appearing to approach asymptotically the open field value.

Similar calculations on systems which include the southern hemisphere as well show only qualitative differences, mainly that the fields extend downwards into the southern hemisphere. The outward bulging characteristic remains the same however.

The important comparison, for our purposes, is shown in Figure 3.4 in which the energy of the magnetic field is plotted as a function of shear angle γ_M (the maximum value of γ). One of the most important results of our program was the discovery that, with spherical geometry, the behavior is quite different from that which we previously found with cylindrical geometry. Whereas, with cylindrical geometry, the total energy rose above the value for the corresponding open-field configuration, this was not the case for spherical geometry: as the shear increased progressively, the magnetic-field energy increased but approached the energy of the open-field configuration asympotically, while in our earlier work with the cylindrical model, the field energy continued increasing linearly past the open field energy.

We spent some time and energy with the aim of determining whether this effect is real or whether it was due to some difference in boundary conditions, error in one of the programs, etc. In order to help resolve these questions, we decided to simulate the cylindrical

model by means of the spherical code. This could be done by considering a ring dipole very close to one of the poles of the sphere. This model substantially reproduced the results of the earlier cylindrical calculations.

This test indicated that there are qualitative differences between the cylindrical and spherical models. Figures 3.5 - 3.8 show results from these runs. The R_{max} and Z_{max} boundaries are conducting in Figures 3.5 - 3.6; the shear angles are π and 2π respectively. In Figure 3.5, the outermost field lines are "flattened" against the boundaries, particularly the R_{max} boundary. This effect is even more pronounced in Figure 3.6, where the fields are strongly influenced by the outer boundaries.

Figure 3.7 shows the shear 2π case with the two outer boundaries opened up. The run associated with this figure was slow to converge, requiring a small relaxation parameter for stability. It is possible that further iteration would see the lines open up further, although we feel the configuration shown is near the final value. Note that the fields open outwards only about ten times the radius of the neutral shear radius. This is in marked contrast to the spherical case, where they extended out several hundred times the scale of the neutral shear line radius. The energy stored in the fields fell somewhat when the boundaries were opened (for the shear of Figure 3.7, it was greater than the completely open field energy). We cannot say whether this is because an appreciable amount of energy was carried across the boundaries when the lines opened up, or because the more open state is simply a state of significantly lower energy. Certainly, the energy versus shear curve

with conducting boundaries increases almost linearly past the completely open field value, in agreement with our earlier result (1972). Figure 3.8 shows the field configuration when the lines are completely open.

This simulation of the earlier cylindrical code with the spherical model indicates that there is a physical difference between the two results and that there are apparently two types of force-free field configurations:

Type 1. For a given magnetic flux distribution on the bounding surface, as the shear increases, the stored energy increases but approaches, as a limiting value, the energy of the corresponding open-field configuration.

Type 2. For given magnetic flux distribution on the bounding surface, the stored energy increases indefinitely as the amount of shear increases. In particular, after a finite amount of shear, the stored energy exceeds the energy of the corresponding open-field configuration.

Nevertheless, it must be emphasized that we have only a presumptive case for this classification: it will be essential to investigate a wider range of models and, even more important, to pin down the precise effect of the outer boundary condition, before this classification can be considered to be established. It remains at this time a possibility that the apparent classification is an artifact of subtle differences in boundary conditions used for different models.

The models of cylindrical topology which we have considered belong to Type 2. The early models of spherical geometry, which we have calculated as part of this program, belong to Type 1. However, when we used the spherical geometry but compressed the field configuration to a small region around one of the poles, the behavior corresponded to that of Type 2.

IV. DISCUSSION

We have found that it is possible to compute force-free field configurations without making the restrictive assumption (adopted in most other work) that α = constant. However, the convergence can become very slow if the magnetic field is highly stressed, and it is clearly desirable to try to find some procedures to speed up convergence. It also would be highly advantageous to pursue these calculations with a more powerful computer.

The most important result of this program is the indication that force-free magnetic-field configurations may be divided into two types, defined at the end of Section III. The evolution of force-free fields of Type 1 would probably not lead to a solar flare. As the stress increases progressively, the field expands and approaches asympotically the open state. Since this open configuration builds up slowly, it seems unlikely that major reconnection would occur. It seems more likely that the field topology would develop into a geometry with a thick current sheet which is fairly stable, such as exists in a coronal streamer. However, it is always possible that a certain disturbance (such as a shock wave) might trigger an instability even in such a current sheet.

By contrast, force-free fields of Type 2 are highly important for the flare problem. They indicate the following sequence of events in an active region leading to a flare: a subphotospheric twisted flux tube erupts to give a bipolar field configuration in an active region. Since it is energetically favorable for the twist to propagate from below the photosphere (where the field is strong) to above the photosphere

(where it is weaker), this will occur, leading to progressive twisting of the force-free field configuration in the atmosphere above the active region. When the field is sufficiently stressed, it contains more energy than does the corresponding open-field configuration. It is therefore either unstable or metastable. The fact that the relaxation calculation is stable (although only marginally so) indicates that such a field configuration is physically stable against small perturbations. It must therefore be metastable, that is, unstable against finite perturbations. A finite perturbation would therefore trigger an eruptive instability converting the closed force-free configuration into the corresponding open-field configuration with a current sheet. The magnetic-field reconnection can occur immediately in this current sheet leading to a solar flare.

To sum up, it seems that the evolution of a force-free field of Type 1 would probably not lead to a flare, whereas the evolution of force-free fields of Type 2 would almost certainly lead to a flare.

It is important to pursue the indication of the existence of two types of force-free field. A wider range of models should be calculated, on a more powerful computer, either removing the outer boundary to very large distances, or finding a method which does not require an outer boundary. For instance, it might be possible to replace the radial variable by $1/r$. However, in this case, it will be essential to study asymptotic forms of force-free magnetic-field configurations to insure that we can properly handle the behavior of the magnetic field in the neighborhood of the singularity $1/r = 0$.

This program demonstrates that one can study the properties of force-free magnetic fields without making the restrictive assumption that α = constant. It also indicates the existence of an important classification of force-free fields. If this classification is valid, it will have an important bearing on flare theory and flare prediction. For instance, one might be able to determine criteria which would enable one to categorize the field produced by an active region as belonging either to Type 1 or Type 2. This would then indicate whether the flare region is or is not likely to produce a flare.

REFERENCES

Anzer, U. 1976, Private communication.

Barnes, C.W. and Sturrock, P.A. 1972, Ap. J. 174, 659.

Furth, H.P., Killeen, J. and Rosenbluth, M.N. 1963, Phys. Fluids 6, 459.

Petschek, H.E. 1964, AAS-NASA Symp. on the Physics of Solar Flares (NASA, SP-50), p. 425.

Schmidt, H.J. 1968, I.A.U. Symp. No. 35, 95.

Spicer, D. 1976, "An Unstable Arch Model of a Solar Flare" (NRL Report 8036)(Naval Research Laboratory: Washington, D.C.).

Sturrock, P.A. and Woodbury, E.T. 1967, Plasma Astrophysics (New York: Academic Press), p. 471.

Sweet, P.A. 1969, Ann. Rev. Astron. Astrophys. 7, 149.

FIGURE CAPTIONS

Figure 3.1. Field configuration for a spherical case with a conducting equator. The neutral shear point occurs at about 65^{o} N. latitude. The radial coordinate is logarithmic and extends to 180 surface radii. Maximum shear for this case is 2.6 radians.

Figure 3.2. The same as Figure 3.1 with maximum shear π radians.

Figure 3.3. The same as Figure 3.2 with maximum shear 2π radians.

Figure 3.4. Curve of stored energy vs maximum shear angle for the case of Figures 3.1 - 3.3. Shown also is the approximate value of the stored energy of the completely open field configuration.

Figure 3.5. Field configuration for a case in which the computational region is restricted to be near the pole, simulating the earlier cylindrical model. The system is nearly "square" (that is a cylinder with radius equal to length) with the neutral shear point occurring at about 1/7 of the outer radius. Maximum shear for this case is π radians.

Figure 3.6. The same as Figure 3.5 with maximum shear 2π radians.

Figure 3.7. The same as Figure 3.6 with the Z_{max} and R_{max} boundaries opened to allow field penetration.

Figure 3.8. The same configuration as Figure 3.5 with completely open

field lines. Here the pattern is current free except along the contour beginning at the neutral shear point, where a current sheet exists.

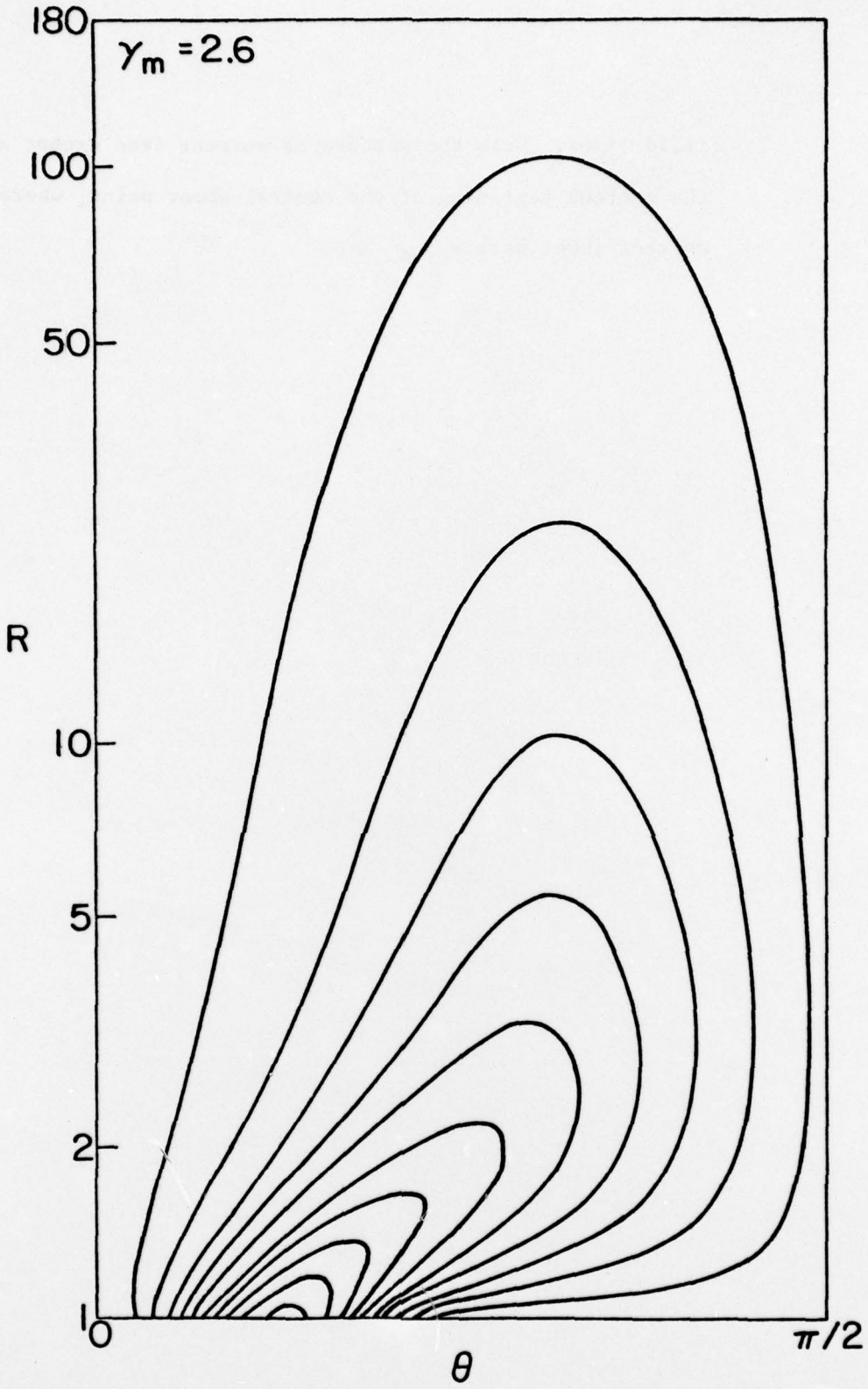

Figure 1

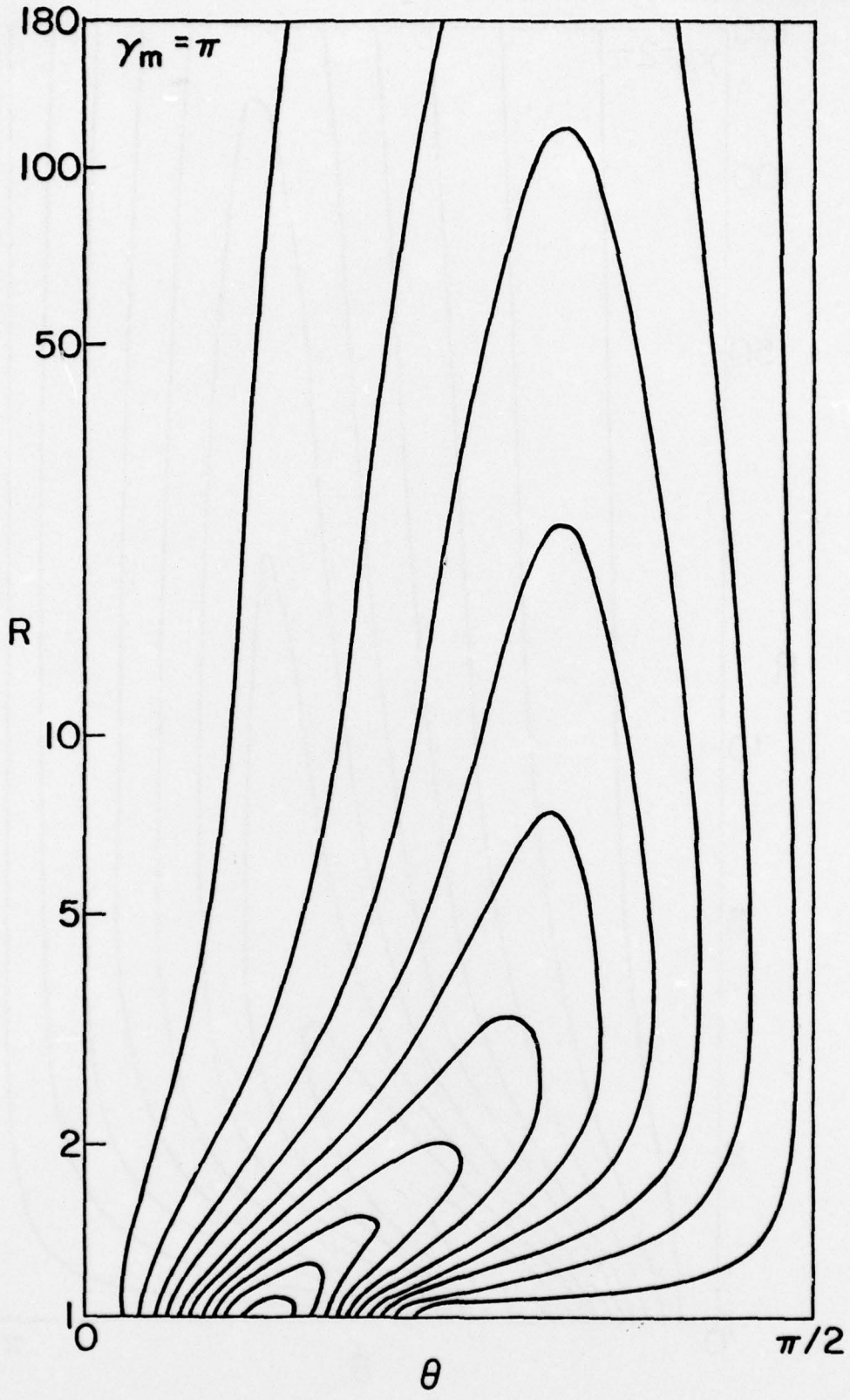

Figure 2

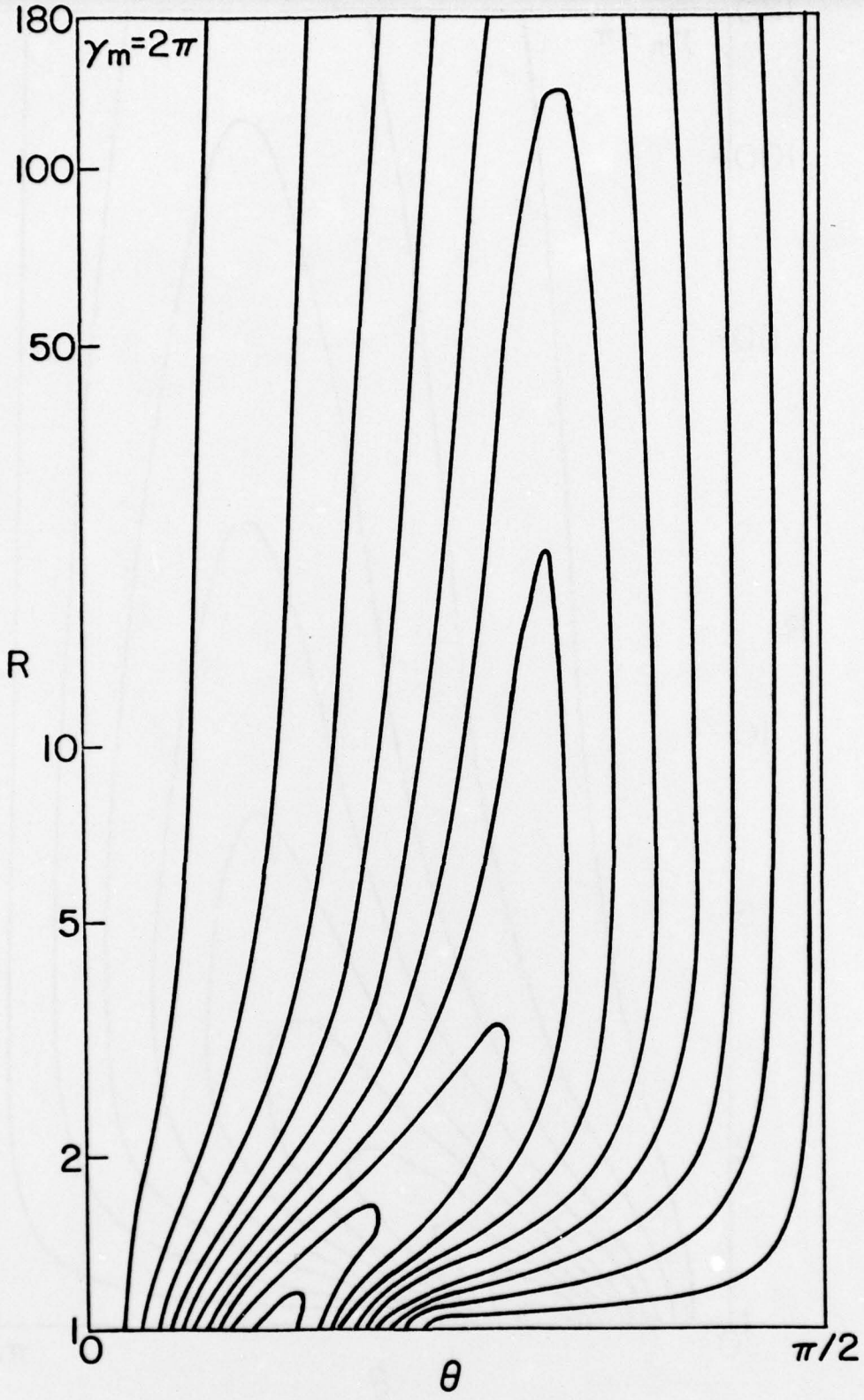

Figure 3

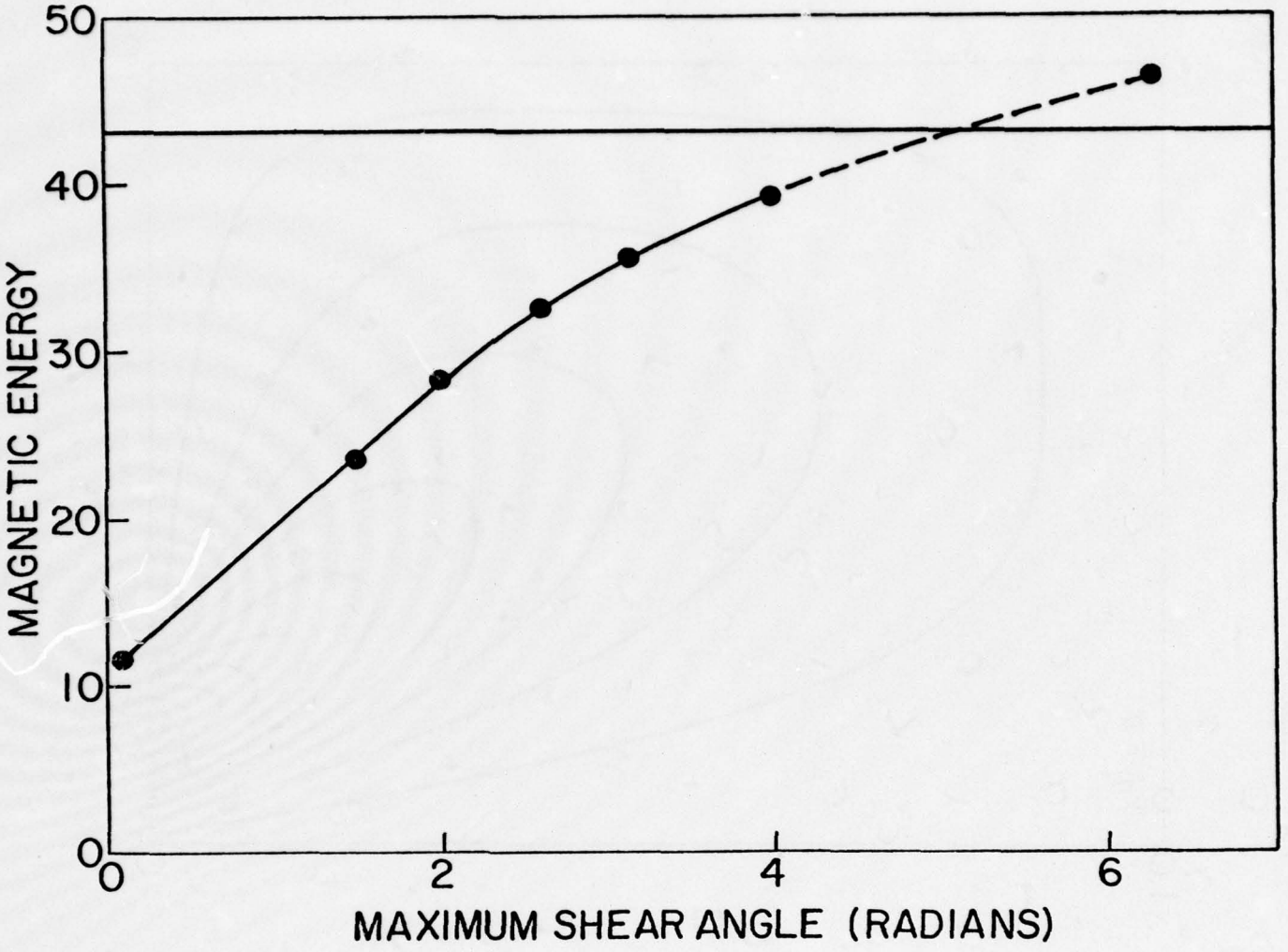
50
40
30
20
10
0
MAGNETIC ENERGY
0
2
4
6
MAXIMUM SHEAR ANGLE (RADIANS)

Figure 4

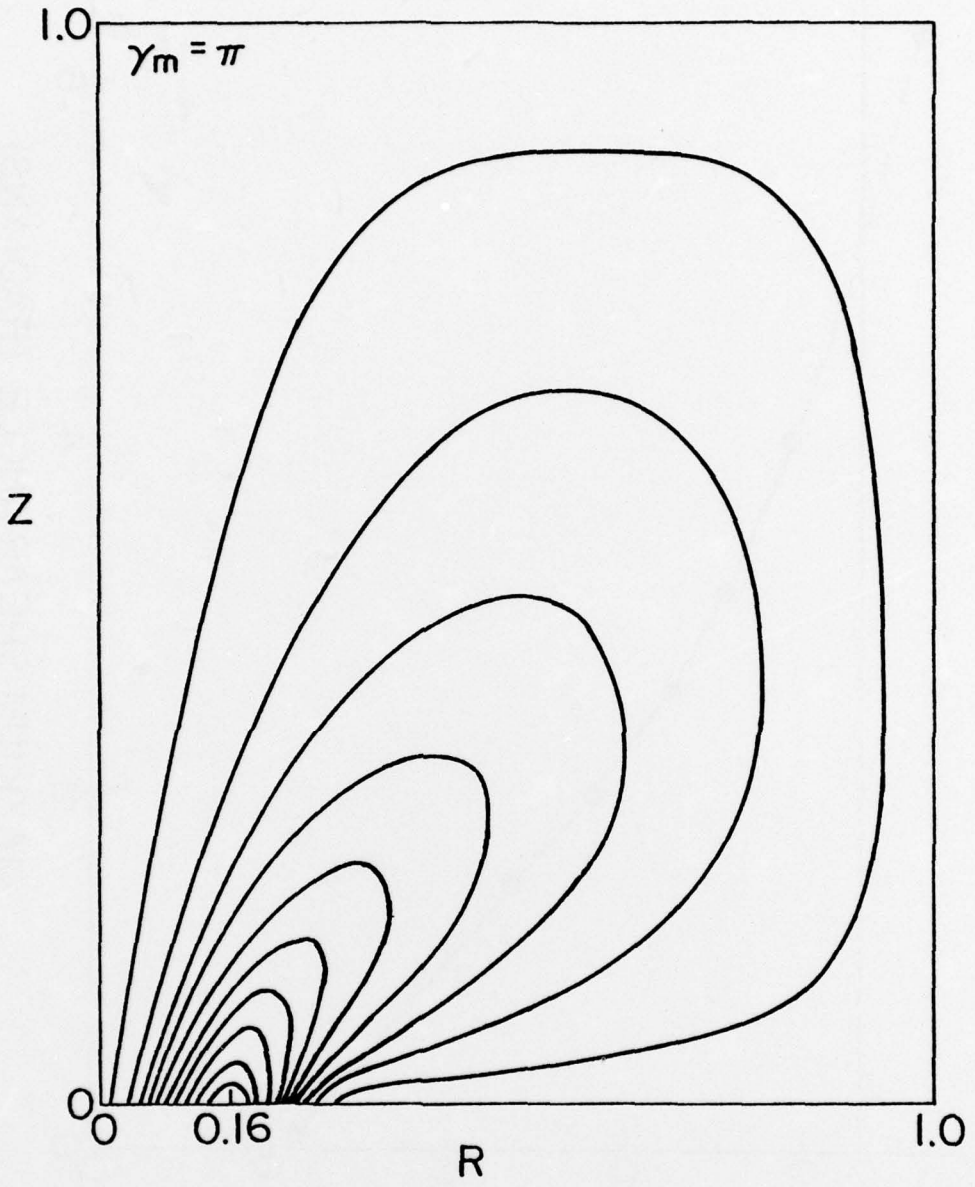

Figure 5

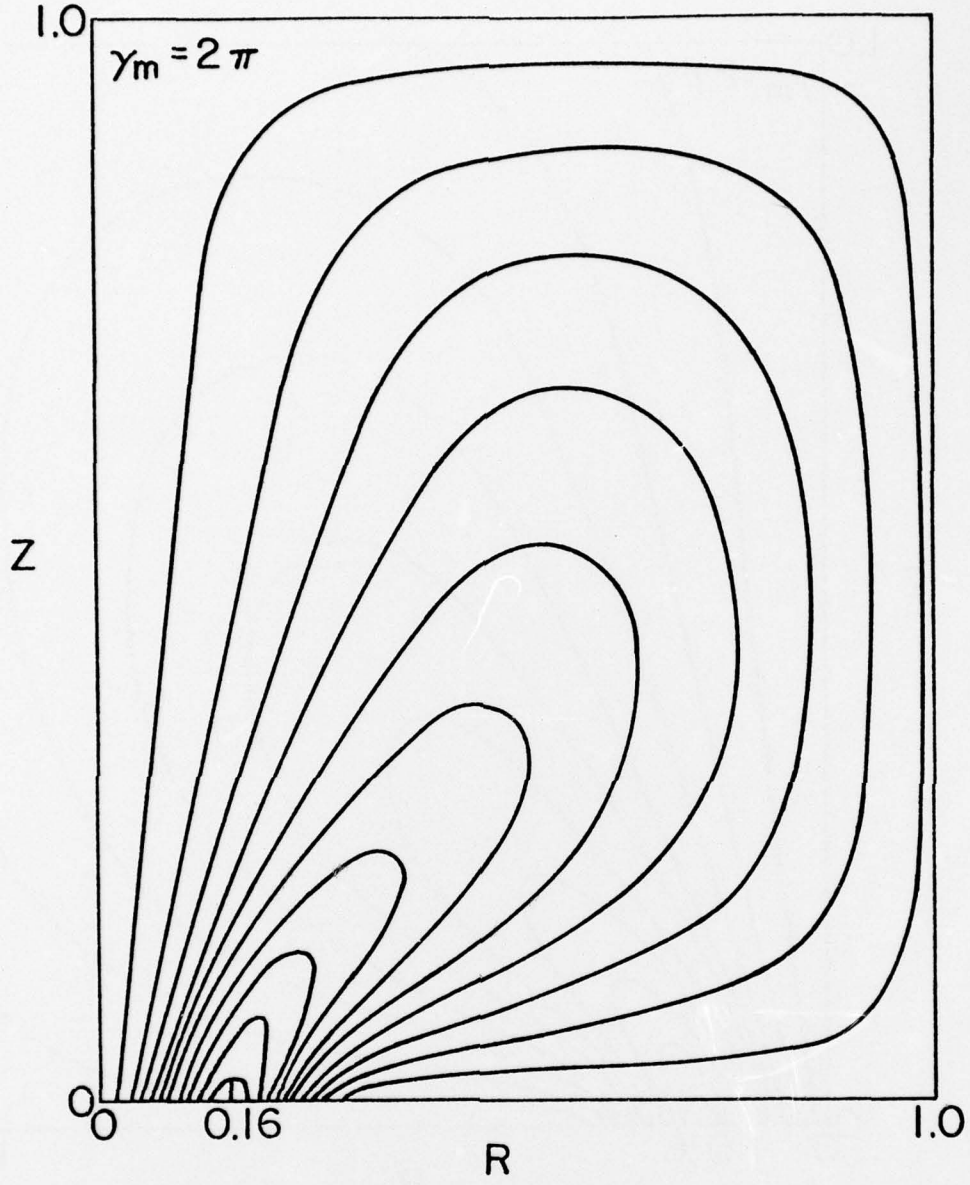

Figure 6

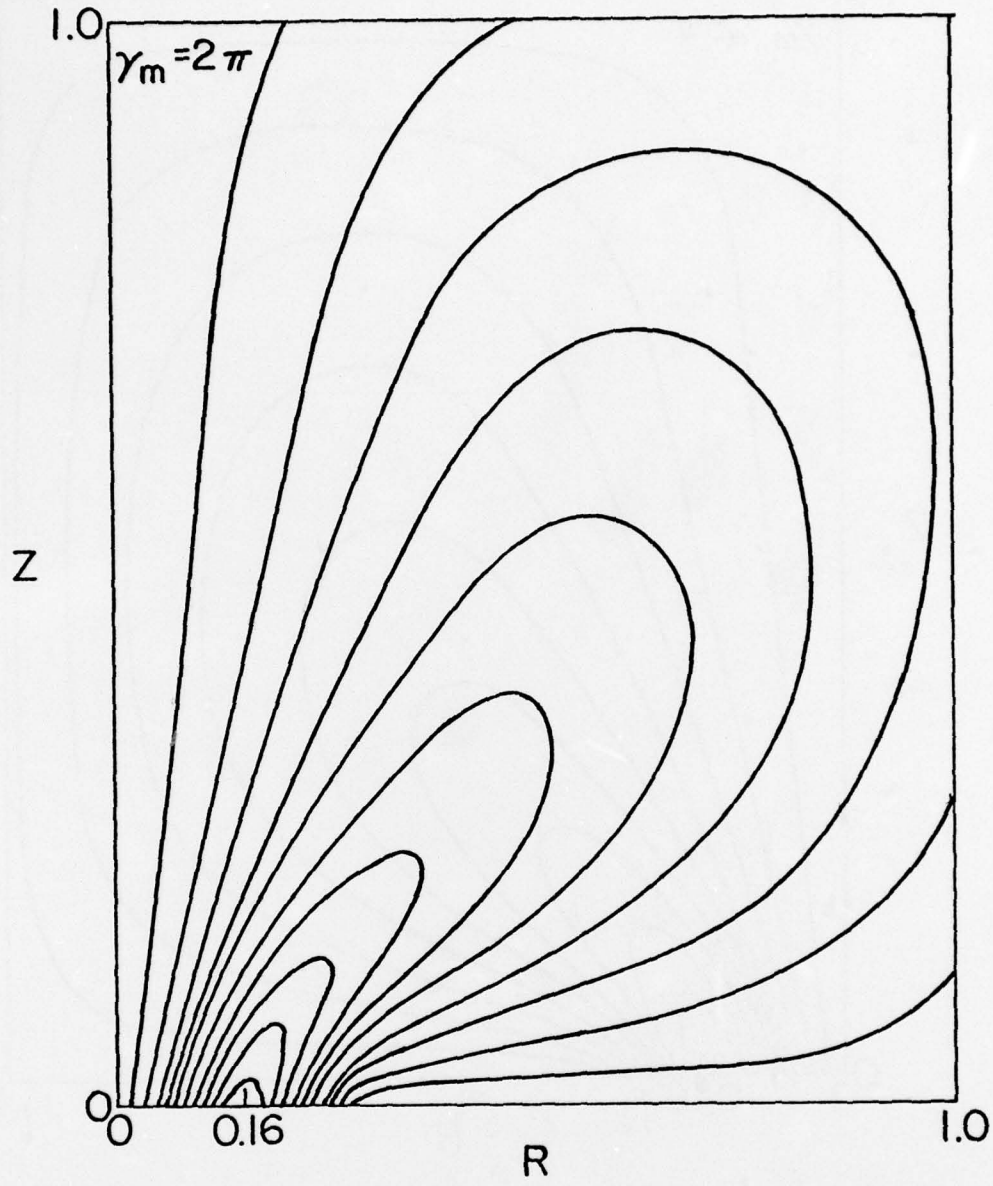

Figure 7

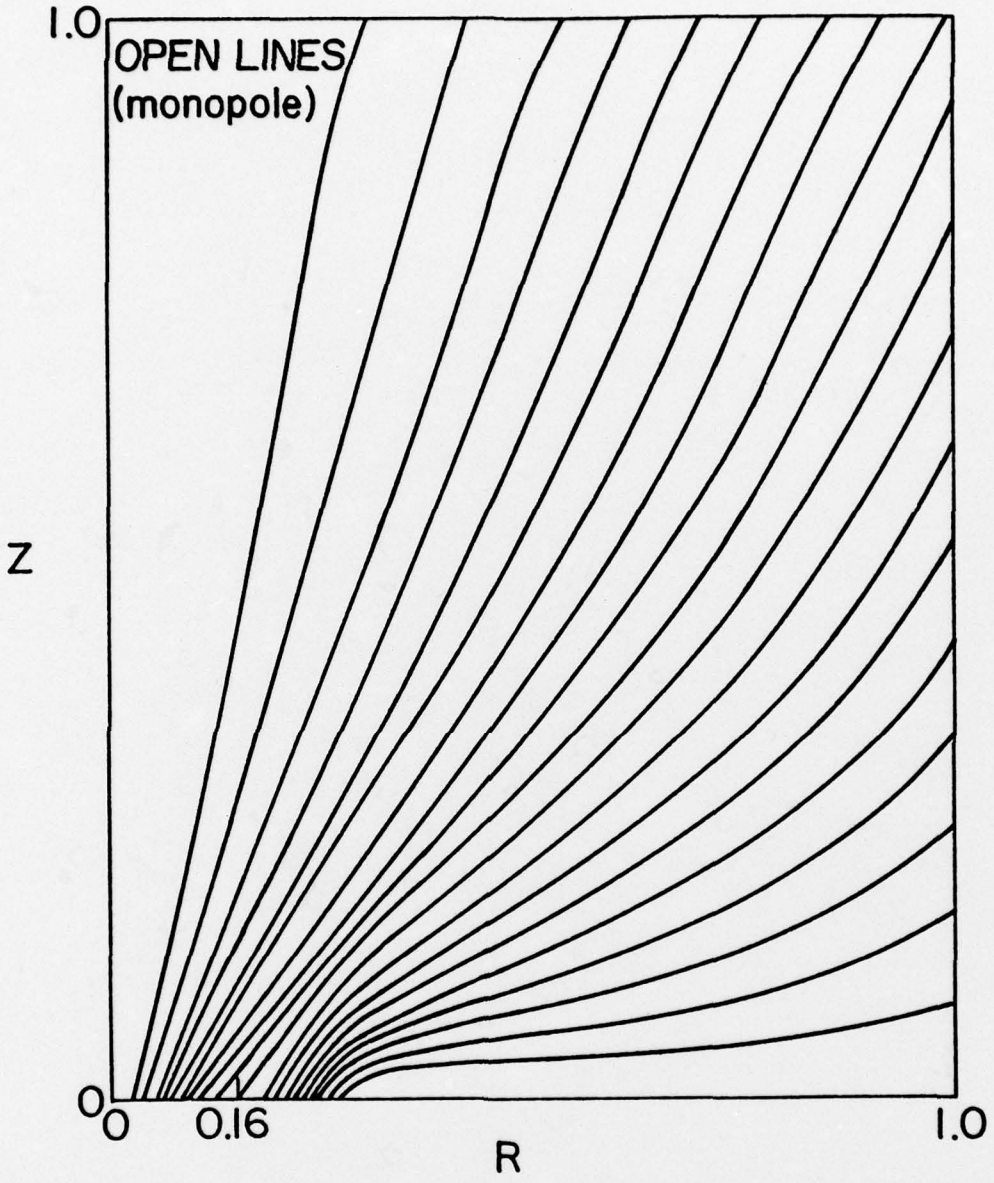

Figure 8